DOI 10.1007/s11141-014-9528-3
Radiophysics and Quantum Electronics, Vol. 57, No. 6, November, 2014
(Russian Original Vol. 57, No. 6, June, 2014)

HIGH-Q QUASISTATIC RESONANCES EXCITED IN A METAMATERIAL SPHERE BY A MERIDIONAL DIPOLE

A. P. Anyutin,[1] D. B. Demin,[2] I. P. Korshunov,[1] *
A. G. Kyurkchan,[1,2] and A. D. Shatrov[1]

UDC 538.566.2+621.372.8

We consider the rigorous problem of excitation of a metamaterial sphere by a meridionally directed electric dipole. High Q-resonances in the low-frequency region are found and studied. The existence conditions of these resonances are established. Frequency-amplitude characteristics of the sphere and the vector scattering patterns at resonant frequencies are calculated. Approximate analytical expressions for resonant frequencies are obtained. The effect of nonresonance field enhancement, which consists in that the scattered field exceeds the primary field in a wide frequency range, is found.

1. INTRODUCTION

Recent years have demonstrated intense advance in electrodynamics of artificial media in which the relative dielectric permittivity ε and the magnetic permeability μ are negative. The first theoretical studies of radiophysical properties of such media were performed by V. G. Veselago [1], and they are often called the Veselago name. Currently, such artificial media are conventionally called metamaterials.

Interaction of an electromagnetic field with metamaterial objects is accompanied by many unusual effects, such as negative refraction, subwave localization, "reversion" of the Doppler and Vavilov–Čerenkov effects, resonance scattering by small bodies, etc. The number of works studying these effects is rather great and continues avalanching (see review works [3–6].

The authors of [7–10] considered two-dimensional problems of excitation of solid and hollow circular metamaterial cylinders by a filamentary source. It was shown that high-Q resonances exist in cylinders with small diameters. In the case of TM-polarization, they occur at the values of ε which are close to -1, and in the case of TE-polarization, at the values of μ which are close to -1.

The purpose of this work is to study low-frequency resonances that occur when a sphere filled with a metamaterial is excited by a meridional dipole.

2. FORMULATION OF THE PROBLEM

Consider the three-dimensional vector problem on excitation of a metamaterial sphere with the negative values of the relative dielectric permittivity ε and the magnetic permeability μ by an elementary electric dipole. It is assumed that the time dependence of the electromagnetic fields is determined by the factor $\exp(i\omega t)$. We use a spherical coordinate system (r, θ, φ). The spatial distribution of the relative material

* korip@ms.ire.rssi.ru

[1] V. A. Kotel'nikov Institute of Radio Engineering and Electronics of the Russian Academy of Sciences, Fryazino; [2] Moscow Technical University of Communication and Informatics, Moscow, Russia. Translated from Izvestiya Vysshikh Uchebnykh Zavedenii, Radiofizika, Vol. 57, No. 6, pp. 507–518, June 2014. Original article submitted November 28, 2013; accepted January 13, 2014.

parameters of the medium is described by the functions

$$\varepsilon(r) = \begin{cases} \varepsilon, & r < a; \\ 1, & r > a, \end{cases} \qquad \mu(r) = \begin{cases} \mu, & r < a; \\ 1, & r > a, \end{cases} \tag{1}$$

where a is the sphere radius.

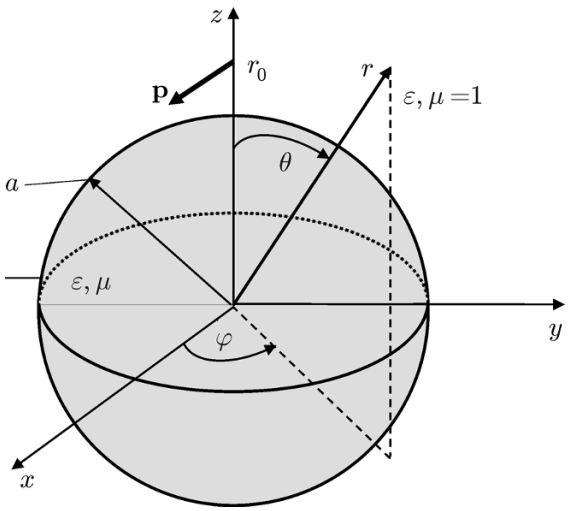

Fig. 1. Geometry of the problem.

The elementary dipole is located at the point $(0, 0, r_0)$ of the Cartesian coordinate system with the origin at the center of the sphere (see Fig. 1). The dipole moment is aligned with the x axis. In this case, the primary field can be expressed in terms of the electric Hertz vector $\mathbf{\Pi}^{(\mathrm{e})}$, which will have the following components in the Cartesian coordinate system:

$$\Pi_x^{(\mathrm{e})} = A \exp(-ikR)/R, \qquad \Pi_y^{(\mathrm{e})} = \Pi_z^{(\mathrm{e})} = 0, \tag{2}$$

where

$$R = \sqrt{r^2 + r_0^2 - 2rr_0 \cos\theta}, \tag{3}$$

$k = \omega\sqrt{\varepsilon_0\mu_0}$, and ε_0 and μ_0 are the dielectric permittivity and magnetic permeability of free space, respectively. The term A in Eq. (2) is specified by the formula

$$A = p/(4\pi\varepsilon_0), \tag{4}$$

where p is the dipole moment.

In the spherical coordinate system, the Hertz vector $\mathbf{\Pi}^{(\mathrm{e})}$ has the components

$$\Pi_r^{(\mathrm{e})} = A\frac{\sin(\theta)\cos(\varphi)}{R}\exp(-ikR), \qquad \Pi_\theta^{(\mathrm{e})} = A\frac{\cos(\theta)\cos(\varphi)}{R}\exp(-ikR),$$
$$\Pi_\varphi^{(\mathrm{e})} = -A\frac{\sin(\varphi)}{R}\exp(-ikR). \tag{5}$$

The electric and magnetic fields are expressed in terms of the vector $\mathbf{\Pi}^{(\mathrm{e})}$ by the well-known formulas

$$\mathbf{E} = (\mathrm{grad}\,\mathrm{div} + k^2)\,\mathbf{\Pi}^{(\mathrm{e})} = \mathrm{rot}\,\mathrm{rot}\,\mathbf{\Pi}^{(\mathrm{e})}, \tag{6}$$

$$\mathbf{H} = \frac{ik}{\zeta_0}\mathrm{rot}\,\mathbf{\Pi}^{(\mathrm{e})}, \tag{7}$$

where

$$\zeta_0 = \sqrt{\mu_0/\varepsilon_0}. \tag{8}$$

In particular, the radial components of the electromagnetic field excited by the source will be determined by the formulas

$$E_r^0 = -A\cos(\varphi)\left\{\frac{1}{r^2}\frac{\partial}{\partial\theta}\left[\sin(\theta)\frac{\partial}{\partial\theta}\frac{\exp(-ikR)}{R}\right] - \frac{1}{r}\cos(\theta)\frac{\partial^2}{\partial r\partial\theta}\frac{\exp(-ikR)}{R}\right.$$
$$\left. + \frac{2}{r}\sin(\theta)\frac{\partial}{\partial r}\frac{\exp(-ikR)}{R} + \frac{1}{r^2}\cos(\theta)\frac{\partial}{\partial\theta}\frac{\exp(-ikR)}{R}\right\}, \tag{9}$$

$$H_r^0 = -A\frac{ik}{\zeta_0}\sin(\varphi)\left[\frac{1}{r}\frac{\partial}{\partial\theta}\frac{\exp(-ikR)}{R}\right]. \tag{10}$$

These components will be needed for formulating the diffraction problem in terms of the Debye potentials.

The problem consists in finding the total field inside the sphere, the scattered field outside the sphere, and the vector scattering pattern from the radial components of the primary field, which are specified by Eqs. (9) and (10).

3. ANALYTICAL SOLUTION OF THE DIFFRACTION PROBLEM BY THE METHOD OF SEPARATION OF VARIABLES

The classical method of solving the problems of diffraction by spherically symmetric bodies consists in using of the Debye potentials (see, e.g., [11, 12]). The electric and magnetic Debye potentials are scalar functions $U^{(\mathrm{e})}(r,\theta,\varphi)$ and $U^{(\mathrm{m})}(r,\theta,\varphi)$, respectively, which satisfy the Helmholtz equation

$$\Delta U + k^2\varepsilon(r)\mu(r)U = 0 \tag{11}$$

inside and outside the sphere and the following boundary conditions at $r = a$:

$$\varepsilon U^{(\mathrm{e})}\Big|_{r=a-0} = U^{(\mathrm{e})}\Big|_{r=a+0}, \qquad \frac{\partial(rU^{(\mathrm{e})})}{\partial r}\Big|_{r=a-0} = \frac{\partial(rU^{(\mathrm{e})})}{\partial r}\Big|_{r=a+0}, \tag{12}$$

$$\mu U^{(\mathrm{m})}\Big|_{r=a-0} = U^{(\mathrm{m})}\Big|_{r=a+0}, \qquad \frac{\partial(rU^{(\mathrm{m})})}{\partial r}\Big|_{r=a-0} = \frac{\partial(rU^{(\mathrm{m})})}{\partial r}\Big|_{r=a+0}. \tag{13}$$

The components of the electromagnetic field are expressed in terms of the Debye potentials by means of the formulas which contain partial derivatives with respect to r, θ, and φ [11, 12]. For example, the radial components are determined as follows:

$$E_r = \left[\frac{\partial^2}{\partial r^2} + k^2\varepsilon(r)\mu(r)\right](rU^{(\mathrm{e})}), \tag{14}$$

$$H_r = \left[\frac{\partial^2}{\partial r^2} + k^2\varepsilon(r)\mu(r)\right](rU^{(\mathrm{m})}). \tag{15}$$

If we use the particular solutions of the Helmholtz equation, which are obtained by the method of separation of variables, as the potentials $U^{(\mathrm{e})}$ and $U^{(\mathrm{m})}$, we then find that in the $r > a$, region

$$U_{lm}(r,\theta,\varphi) = \left\{\begin{array}{c} j_l(kr) \\ h_l^{(2)}(kr) \end{array}\right\} P_l^m(\cos\theta)\exp(im\varphi). \tag{16}$$

Here, j_l and $h_l^{(2)}$ are spherical Bessel and Hankel functions, respectively, and P_l^m are associated Legendre polynomials. Potentials (16) give rise to spherical vector multipole modes of the electric and magnetic types.

The problem of diffraction of a single mode $j_l(kr)P_l^m(\cos\theta)\exp(im\varphi)$ by the sphere has a simple solution: in the region $r > a$, the scattered field is represented as the single spherical mode $R_l h_l^{(2)}(kr)P_l^m(\cos\theta)\times \exp(im\varphi)$ with a simple explicit formula for the reflection coefficient R_l (Mie coefficient). Thus, the main stage of solving the problem of diffraction by a sphere consists in expansion of the incident field (Eqs. (9) and 10)) over the spherical vector multipole modes.

Then we transform Eq. (9). It follows from Eq. (3) that

$$\frac{\partial}{\partial r}\left[\frac{\exp(-ikR)}{R}\right] = \left[\frac{\partial}{\partial R}\frac{\exp(-ikR)}{R}\right]\frac{r - r_0\cos\theta}{R}, \tag{17}$$

$$\frac{\partial}{\partial r_0}\left[\frac{\exp(-ikR)}{R}\right] = \left[\frac{\partial}{\partial R}\frac{\exp(-ikR)}{R}\right]\frac{r_0 - r\cos\theta}{R}, \tag{18}$$

$$\frac{\partial}{\partial \theta}\left[\frac{\exp(-ikR)}{R}\right] = \left[\frac{\partial}{\partial R}\frac{\exp(-ikR)}{R}\right]\frac{r r_0 \sin\theta}{R}. \tag{19}$$

The following relationships follow from Eqs. (17)–(19):

$$\frac{\partial}{\partial r_0}\left[\frac{\exp(-ikR)}{R}\right] = \frac{1}{r}\sin(\theta)\frac{\partial}{\partial \theta}\left[\frac{\exp(-ikR)}{R}\right] - \cos(\theta)\frac{\partial}{\partial r}\left[\frac{\exp(-ikR)}{R}\right], \tag{20}$$

$$\frac{1}{r_0}\frac{\partial}{\partial \theta}\left[\frac{\exp(-ikR)}{R}\right] = \sin(\theta)\frac{\partial}{\partial r}\left[\frac{\exp(-ikR)}{R}\right] + \frac{1}{r}\cos(\theta)\frac{\partial}{\partial \theta}\left[\frac{\exp(-ikR)}{R}\right]. \tag{21}$$

Equations (20) and (21) allow one to represent Eq. (9) in a more concise form

$$E_r^0 = -A\cos(\varphi)\left\{\frac{1}{r_0 r}\frac{\partial^2}{\partial\theta\partial r_0}\left[r_0\frac{\exp(-ikR)}{R}\right]\right\}. \tag{22}$$

The following Debye potentials correspond to the incident field in the region $a < r < r_0$:

$$rU^{(\mathrm{e})}(r,\theta,\varphi) = \frac{Ai}{r_0}\cos(\varphi)\sum_{l=1}^{\infty}\frac{2l+1}{l\,(l+1)}\bar{h}_l^{(2)\prime}(kr_0)\bar{j}_l(kr)P_l^1(\cos\theta), \tag{23}$$

$$rU^{(\mathrm{m})}(r,\theta,\varphi) = -\frac{A}{\eta_0 r_0}\sin(\varphi)\sum_{l=1}^{\infty}\frac{2l+1}{l\,(l+1)}\bar{h}_l^{(2)}(kr_0)\bar{j}_l(kr)P_l^1(\cos\theta), \tag{24}$$

where $\bar{j}_l(kr)$ and $\bar{h}_l^{(2)}(kr_0)$ are Riccati–Bessel and Riccati–Hankel functions

$$\bar{j}_l(kr) = krj_l(kr), \qquad \bar{h}_l^{(2)}(kr) = krh_l^{(2)}(kr). \tag{25}$$

The prime in Eq. (23) denotes differentiation with respect to the argument.

In order to verify that expansions (23) and (24) are correct, it is sufficient to apply the operator $\partial^2/\partial r^2 + k^2$ to them and compare the obtained results with Eqs. (10) and (22). The following relationships [13] will be needed for this procedure:

$$\frac{\exp(-ikR)}{R} = -ik\sum_{l=0}^{\infty}(2l+1)\,j_l(kr)h_l^{(2)}(kr_0)P_l(\cos\theta), \qquad r < r_0, \tag{26}$$

$$\frac{\mathrm{d}}{\mathrm{d}\theta}P_l(\cos\theta) = P_l^1(\cos\theta), \tag{27}$$

$$\left(\frac{\mathrm{d}^2}{\mathrm{d}r^2} + k^2\right)\bar{j}_l(kr) = \frac{l\,(l+1)}{r^2}\bar{j}_l(kr). \tag{28}$$

Using expansions (23) and (24), we use the standard procedure to obtain formulas for the Debye potentials that describe the scattered field ($r > a$):

$$rU^{(\mathrm{e})} = \frac{Ai}{r_0}\cos(\varphi)\sum_{l=1}^{\infty}\frac{2l+1}{l\,(l+1)}R_l^{(\mathrm{e})}\bar{h}_l^{(2)\prime}(kr_0)\bar{h}_l^{(2)}(kr)P_l^1(\cos\theta), \tag{29}$$

$$rU^{(\mathrm{m})} = -\frac{A}{\zeta_0 r_0}\sin(\varphi)\sum_{l=1}^{\infty}\frac{2l+1}{l\,(l+1)}R_l^{(\mathrm{m})}\bar{h}_l^{(2)}(kr_0)\bar{h}_l^{(2)}(kr)P_l^1(\cos\theta), \tag{30}$$

where

$$R_l^{(\mathrm{e})} = -\frac{\bar{j}_l'(ka)\bar{j}_l(Nka) - N\bar{j}_l(ka)\bar{j}_l'(Nka)/\varepsilon}{\bar{h}_l^{(2)\prime}(ka)\bar{j}_l(Nka) - N\bar{h}_l^{(2)}(ka)\bar{j}_l'(Nka)/\varepsilon}, \tag{31}$$

$$R_l^{(\mathrm{m})} = -\frac{\bar{j}_l'(ka)\bar{j}_l(Nka) - N\bar{j}_l(ka)\bar{j}_l'(Nka)/\mu}{\bar{h}_l^{(2)\prime}(ka)\bar{j}_l(Nka) - N\bar{h}_l^{(2)}(ka)\bar{j}_l'(Nka)/\mu}, \tag{32}$$

$$N = \sqrt{\varepsilon\mu}. \tag{33}$$

The components of the electromagnetic field are expressed in terms of the Debye potentials [11], namely,

$$E_\theta = \frac{1}{r}\frac{\partial^2(rU^{(\mathrm{e})})}{\partial r\,\partial\theta} - \frac{ik\zeta_0\mu(r)}{\sin\theta}\frac{\partial U^{(\mathrm{m})}}{\partial\varphi}, \tag{34}$$

$$E_\varphi = \frac{1}{r\sin\theta}\frac{\partial^2(rU^{(\mathrm{e})})}{\partial r\,\partial\varphi} + ik\zeta_0\mu(r)\frac{\partial U^{(\mathrm{m})}}{\partial\theta}. \tag{35}$$

Let us denote the components of the vector scattering pattern as $F_\theta(\theta,\varphi)$ and $F_\varphi(\theta,\varphi)$

$$E_\theta \sim F_\theta\frac{\exp(-ikr)}{r}, \qquad E_\varphi \sim F_\varphi\frac{\exp(-ikr)}{r}, \qquad kr\to\infty. \tag{36}$$

Then, from Eqs. (29), (30), and (34)–(36), we obtain the following formulas for the components of the vector scattering pattern:

$$F_\theta = Ak^2\frac{\cos(\varphi)}{kr_0}\sum_{l=1}^{\infty} i^l\frac{2l+1}{l\,(l+1)}\left[iR_l^{(\mathrm{e})}\bar{h}_l^{(2)\prime}(kr_0)\frac{\mathrm{d}P_l^1(\cos\theta)}{\mathrm{d}\theta} - R_l^{(\mathrm{m})}\bar{h}_l^{(2)}(kr_0)\frac{P_l^1(\cos\theta)}{\sin\theta}\right], \tag{37}$$

$$F_\varphi = -Ak^2\frac{\sin(\varphi)}{kr_0}\sum_{l=1}^{\infty} i^l\frac{2l+1}{l\,(l+1)}\left[iR_l^{(\mathrm{e})}\bar{h}_l^{(2)\prime}(kr_0)\frac{P_l^1(\cos\theta)}{\sin\theta} - R_l^{(\mathrm{m})}\bar{h}_l^{(2)}(kr_0)\frac{\mathrm{d}P_l^1(\cos\theta)}{\mathrm{d}\theta}\right]. \tag{38}$$

In Eqs. (37) and (38), we single out the term Ak^2 which is equal to the amplitude of the radiation patterns F_θ^0 and F_φ^0 of the primary field:

$$F_\theta^0 = Ak^2\cos(\varphi)\cos(\theta)\exp(ikr_0\cos\theta), \tag{39}$$

$$F_\varphi^0 = -Ak^2\sin(\varphi)\exp(ikr_0\cos\theta). \tag{40}$$

At $kr_0\to\infty$, Eqs. (37) and (38) go over to the well-known formulas for the scattering pattern of a plane wave [11].

4. LOW-FREQUENCY RESONANCES

The quantities $R_l^{(\mathrm{e})}$ and $R_l^{(\mathrm{m})}$ determined by Eqs. (31) and (32), respectively, contain resonance denominators. At $ka \ll 1$ and $Nka \ll 1$, the imaginary parts of these denominators exceed their real parts significantly. Vanishing the imaginary parts leads to resonances.

For example, let us study the formula for $R_l^{(\mathrm{e})}$. The equation for the resonant frequencies of the electric-type modes has the form

$$\bar{n}_l'(ka)\bar{j}_l(Nka) - N\bar{n}_l(ka)\bar{j}_l'(Nka)/\varepsilon = 0, \tag{41}$$

where $\bar{n}_l(ka)$ is a Riccati–Neumann function.

Using asymptotic expansions of the functions $\bar{j}_l(Nka)$ and $\bar{n}_l(ka)$ for small values of their arguments,

we obtain the following expressions for finding the resonant frequencies from Eq. (41):

$$(ka)^2 = \frac{l + (l+1)/\varepsilon}{\mu/(2l+3) + 1/(2l-1)}, \qquad l \geq 1. \tag{42}$$

It follows from Eq. (42) that for the electric-type modes, low-frequency resonances occur in the case when the dielectric permittivity of the sphere is close to the quantity given by the formula

$$\varepsilon = -(l+1)/l, \qquad l \geq 1. \tag{43}$$

For example, it follows from Eq. (42) that for

$$l = 3, \qquad \varepsilon = -1.335, \qquad \mu = -1, \tag{44}$$

the resonant frequency is determined by the formula

$$ka \approx 0.2, \tag{45}$$

while for

$$l = 4, \qquad \varepsilon = -1.252, \qquad \mu = -1, \tag{46}$$

by the formula

$$ka \approx 0.35. \tag{47}$$

It follows from Eqs. (37) and (38) that at the resonant frequencies, the scattering pattern will be described approximately by the functions

$$F_\theta \sim \cos(\varphi)\frac{\mathrm{d}P_l^1(\cos\theta)}{\mathrm{d}\theta}, \qquad F_\varphi \sim -\sin(\varphi)\frac{P_l^1(\cos\theta)}{\sin\theta}. \tag{48}$$

One can consider low-frequency resonances of the magnetic-type modes in a similar way. The corresponding equation for the resonant frequencies has the form

$$\bar{n}_l'(ka)\bar{j}_l(Nka) - N\bar{n}_l(ka)\bar{j}_l'(Nka)/\mu = 0. \tag{49}$$

This equation differs from Eq. (41) in that the quantities ε and μ are interchanged.

5. METHOD OF DIAGRAM EQUATIONS

The problem of description of wave diffraction by magnetodielectric scatterers with fairly arbitrary geometry can efficiently be solved by using the method of diagram equations [14, 15]. According to this method, the initial boundary value problem is reduced to solving a system of algebraic equations for the coefficients of expansion of the external scattered field ($\mathbf{E}^1$, $\mathbf{H}^1$) and the internal field ($\mathbf{E}^{\mathrm{i}}$, $\mathbf{H}^{\mathrm{i}}$) into series in terms of the spherical wave harmonics:

$$\mathbf{E}^1 = \sum_{n=1}^{\infty}\sum_{m=-n}^{n}\Big\{a_{nm}\left[\boldsymbol{\nabla}\times\boldsymbol{\nabla}\times(\mathbf{r}\psi_n^m)\right] - ik\zeta_0 b_{nm}\left[\boldsymbol{\nabla}\times(\mathbf{r}\psi_n^m)\right]\Big\}, \tag{50}$$

$$\mathbf{H}^1 = \sum_{n=1}^{\infty}\sum_{m=-n}^{n}\Big\{\frac{ik}{\zeta_0}a_{nm}\left[\boldsymbol{\nabla}\times(\mathbf{r}\psi_n^m)\right] + b_{nm}\left[\boldsymbol{\nabla}\times\boldsymbol{\nabla}\times(\mathbf{r}\psi_n^m)\right]\Big\}, \tag{51}$$

$$\mathbf{E}^{\mathrm{i}} = \sum_{n=1}^{\infty}\sum_{m=-n}^{n}\Big\{a_{nm}^{\mathrm{i}}\left[\boldsymbol{\nabla}\times\boldsymbol{\nabla}\times(\mathbf{r}\chi_{in}^m)\right] - ik\zeta_0\mu b_{nm}^{\mathrm{i}}\left[\boldsymbol{\nabla}\times(\mathbf{r}\chi_n^m)\right]\Big\}, \tag{52}$$

$$\mathbf{H}^{\mathrm{i}} = \sum_{n=1}^{\infty} \sum_{m=-n}^{n} \left\{ \frac{ik\varepsilon}{\zeta_0} a_{nm}^{\mathrm{i}} \left[\boldsymbol{\nabla} \times (\mathbf{r}\chi_{in}^m) \right] + b_{nm}^{\mathrm{i}} \left[\boldsymbol{\nabla} \times \boldsymbol{\nabla} \times (\mathbf{r}\chi_n^m) \right] \right\}. \tag{53}$$

In the presented relationships,

$$\psi_n^m = h_n^{(2)}(kr) P_n^m(\cos\theta) \exp(im\varphi), \qquad \chi_{in}^m = j_n(Nkr) P_n^m(\cos\theta) \exp(im\varphi), \tag{54}$$

and a_{nm}, b_{nm}, a_{nm}^i, and b_{nm}^i are the undetermined coefficients of expansions of the diffracted and internal fields, respectively.

The above-mentioned algebraic system of equations has the following form [14, 15]:

$$a_{nm} = \sum_{q=1}^{\infty} \sum_{p=-q}^{q} (G_{nm,qp}^{13} a_{qp}^{\mathrm{i}} + G_{nm,qp}^{14} b_{qp}^{\mathrm{i}}), \qquad b_{nm} = \sum_{q=1}^{\infty} \sum_{p=-q}^{q} (G_{nm,qp}^{23} a_{qp}^{\mathrm{i}} + G_{nm,qp}^{24} b_{qp}^{\mathrm{i}}), \tag{55}$$

$$a_{nm}^{\mathrm{i}} = a_{nm}^0 + \sum_{q=1}^{\infty} \sum_{p=-q}^{q} (G_{nm,qp}^{31} a_{qp} + G_{nm,qp}^{32} b_{qp}), \quad b_{nm}^{\mathrm{i}} = b_{nm}^0 + \sum_{q=1}^{\infty} \sum_{p=-q}^{q} (G_{nm,qp}^{41} a_{qp} + G_{nm,qp}^{42} b_{qp}) \tag{56}$$

for $n = 1, 2, \ldots$ and $|m| \le n$. The relationships for the matrix elements $G_{nm,qp}^{ij}$ and the free terms a_{nm}^0 and b_{nm}^0 are presented in [14, 15]. In the special case of a spherical scatterer, we have

$$\begin{gathered}
G_{nm,qm}^{13} = i\delta_{qn} \left[\bar{j}_n(ka) \bar{j}_q'(Nka) - \varepsilon \bar{j}_n'(ka) \bar{j}_q(Nka)/N \right], \\
G_{nm,qm}^{14} = 0, \qquad G_{nm,qm}^{23} = 0, \\
G_{nm,qm}^{24} = i\delta_{qn} \left[\bar{j}_n(ka) \bar{j}_q'(Nka) - \mu \bar{j}_n'(ka) \bar{j}_q(Nka)/N \right], \\
G_{nm,qm}^{31} = -i\delta_{qn} \left[\bar{h}_q^{(2)\prime}(ka) \bar{h}_n^{(2)}(Nka) - N \bar{h}_q^{(2)}(ka) \bar{h}_n^{(2)\prime}(Nka)/\varepsilon \right], \\
G_{nm,qm}^{32} = 0, \qquad G_{nm,qm}^{41} = 0, \\
G_{nm,qm}^{42} = -i\delta_{qn} \left[\bar{h}_q^{(2)\prime}(ka) \bar{h}_n^{(2)}(Nka) - N \bar{h}_q^{(2)}(ka) \bar{h}_n^{(2)\prime}(Nka)/\mu \right],
\end{gathered} \tag{57}$$

where δ_{qn} is the Kronecker delta.

As a result, the solution of the system of Eqs. (55) and (56) has the following form:

$$a_{nm} = \frac{G_{nm,nm}^{13} a_{nm}^0}{1 - G_{nm,nm}^{13} G_{nm,nm}^{31}}, \qquad b_{nm} = \frac{G_{nm,nm}^{24} b_{nm}^0}{1 - G_{nm,nm}^{24} G_{nm,nm}^{42}}, \tag{58}$$

$$a_{nm}^{\mathrm{i}} = a_{nm}^0 + G_{nm,nm}^{31} a_{nm}, \qquad b_{nm}^{\mathrm{i}} = b_{nm}^0 + G_{nm,nm}^{42} b_{nm}. \tag{59}$$

In the case where the primary field $(\mathbf{E}^0, \mathbf{H}^0)$ is produced by the electric dipole located at the z axis and aligned with the x axis, the free terms a_{nm}^0 and b_{nm}^0 differ from zero only for $m = \pm 1$. In this case,

$$\begin{aligned}
a_{n,\pm1}^0 = -\frac{\zeta_0 N_{n,\pm1} a}{16\pi} \int_0^{\pi} \Bigg\{ & \frac{N}{\varepsilon} \bar{h}_n^{(2)\prime}(Nka) \left[\tilde{H}_\varphi^0(a,\theta) \sin\theta \frac{\mathrm{d}P_n^{\pm1}(\cos\theta)}{\mathrm{d}\theta} - \tilde{H}_\theta^0(a,\theta) P_n^{\pm1}(\cos\theta) \right] \\
& + \frac{1}{k} \bar{h}_n^{(2)}(Nka) \left[-\tilde{E}_\varphi^0(a,\theta) P_n^{\pm1}(\cos\theta) + \tilde{E}_\theta^0(a,\theta) \sin\theta \frac{\mathrm{d}P_n^{\pm1}(\cos\theta)}{\mathrm{d}\theta} \right] \Bigg\} \mathrm{d}\theta,
\end{aligned} \tag{60}$$

$$b_{n,\pm1}^0 = \frac{N_{n,\pm1} a}{16\pi} \int_0^{\pi} \left\{ \frac{N}{k\mu} \bar{h}_n^{(2)\prime}(Nka) \left[-\tilde{E}_\varphi^0(a,\theta) \sin\theta \frac{\mathrm{d}P_n^{\pm1}(\cos\theta)}{\mathrm{d}\theta} + \tilde{E}_\theta^0(a,\theta) P_n^{\pm1}(\cos\theta) \right] \right.$$

$$+\bar{h}_n^{(2)}(Nka)\left[-\tilde{H}_\varphi^0(a,\theta)P_n^{\pm1}(\cos\theta)+\tilde{H}_\theta^0(a,\theta)\sin\theta\frac{\mathrm{d}P_n^{\pm1}(\cos\theta)}{\mathrm{d}\theta}\right]\Bigg\}\mathrm{d}\theta, \quad (61)$$

where

$$P_n^{-1}=-\frac{1}{n\,(n+1)}P_n^1, \qquad N_{n,1}=\frac{2n+1}{[n\,(n+1)]^2}, \qquad N_{n,-1}=N_{n,1}\,[n\,(n+1)]^2,$$

$$H_\theta^0=-\frac{\sin\varphi}{4\pi}\tilde{H}_\theta^0, \qquad \tilde{H}_\theta^0(r,\theta)=(r-r_0\cos\theta)\left(\frac{ik}{R^2}+\frac{1}{R^3}\right)\exp(-ikR),$$

$$H_\varphi^0=\frac{\cos\varphi}{4\pi}\tilde{H}_\varphi^0, \qquad \tilde{H}_\varphi^0(r,\theta)=(r_0-r\cos\theta)\left(\frac{ik}{R^2}+\frac{1}{R^3}\right)\exp(-ikR),$$

$$E_\theta^0=\frac{\zeta_0}{ik}\frac{\cos\varphi}{4\pi}\tilde{E}_\varphi^0,$$

$$\tilde{E}_\theta^0(r,\theta)=\left[2\cos\theta\left(\frac{ik}{R^2}+\frac{1}{R^3}\right)+(r_0-r\cos\theta)\,(r-r_0\cos\theta)\left(-\frac{k^2}{R^3}+\frac{3ik}{R^4}+\frac{3}{R^5}\right)\right]\exp(-ikR),$$

$$E_\varphi^0=\frac{\zeta_0}{ik}\frac{\sin\varphi}{4\pi}\tilde{E}_\varphi^0, \qquad \tilde{E}_\varphi^0(r,\theta)=\left[\left(\frac{ik}{R^2}+\frac{1}{R^3}\right)-\frac{k^2}{R}\right]\exp(-ikR). \quad (62)$$

Here, the adopted normalization of the fields $\mathbf{E}^0$ and $\mathbf{H}^0$ corresponds to the unit moment of the dipole current. Equations (62) will coincide with the formulas for the primary field, which are given in Sec. 2, if one assumes that the dipole moment is equal to $p=(i\omega)^{-1}$. In this case, $A=\zeta_0\,(4\pi ik)^{-1}$.

6. NUMERICAL RESULTS

The numerical results presented below are obtained by using both the method of diagram equations and Eqs. (37) and (38). They are in full agreement with each other.

In what follows, by the scattering patterns F_θ and F_φ we mean the dimensionless quantities which are determined by Eqs. (37) and (38) if one omits therein the dimensional term Ak^2, which is equal to the maximum amplitude of the radiation patterns F_θ^0 and F_φ^0 of the primary field.

First, we study the dependence of the absolute value of the scattering-pattern component $F_\theta(\pi,0)$ on the parameter ka. We will call this dependence the frequency-amplitude characteristic of the sphere and neglect the frequency dispersion of the metamaterial. In all calculations, the coordinate r_0 of the source was assumed equal to $1.2a$.

Figure 2 shows the frequency-amplitude characteristics of a sphere for two sets of values of ε and μ, which are specified by Eqs. (44) and (46) (curves *1* and *2*, respectively). Dependences *1* and *2* have the resonance character. The resonant frequencies are found from the relationships

$$ka_3=0.20468710\ldots, \quad (63)$$

$$ka_4=0.349352769\ldots\,. \quad (64)$$

The values of the resonant frequencies obtained from Eqs. (63) and (64) agree well with the values found from Eqs. (45) and (47), which are obtained from approximate formula (42). The resonance Q-factors are estimated as $Q_3\sim5\cdot10^4$ and $Q_4\sim7\cdot10^5$. Since the thermal loss in the medium is not allowed for in the calculations presented, the resonance Q-factors are determined only by the radiation loss. The latter turned out to be rather low, which required calculation of the resonant frequencies with the high accuracy used in Eqs. (63) and (64).

To study the influence of the thermal loss on the resonance Q-factors, we used the method of diagram equations. Figure 3 shows a set of curves which describe the frequency-amplitude characteristics of the sphere near the resonant frequency ka_3 for various values of the quantity $\nu=-\mathrm{Im}\,\varepsilon$ that determines the thermal

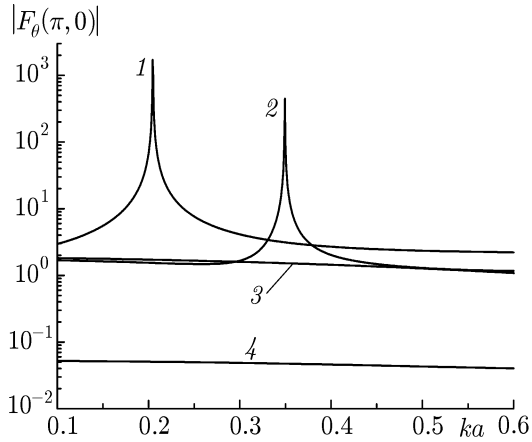

Fig. 2. Frequency-amplitude characteristic $F_\theta(\pi,0)$ of the sphere with $\varepsilon = -1.335$ and $\mu = -1$ (curve *1*), $\varepsilon = -1.252$ and $\mu = -1$ (*2*), $\varepsilon = -1.3$ and $\mu = -1$ (*3*), and $\varepsilon = 1.3$ and $\mu = 1$ (*4*).

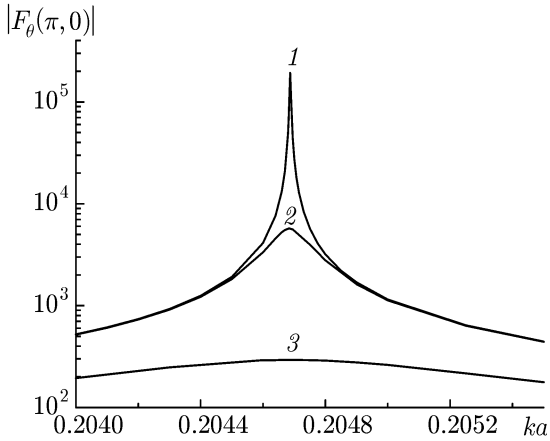

Fig. 3. Frequency-amplitude characteristic $F_\theta(\pi,0)$ of the sphere with $\varepsilon = -1.335$ and $\mu = -1$ near the dimensionless resonant frequency $ka_3 = 0.2046\ldots$ for different dielectric-loss values: curves *1*, *2* and *3* correspond to $\nu = 10^{-9}$, 10^{-6}, and 10^{-5}, respectively.

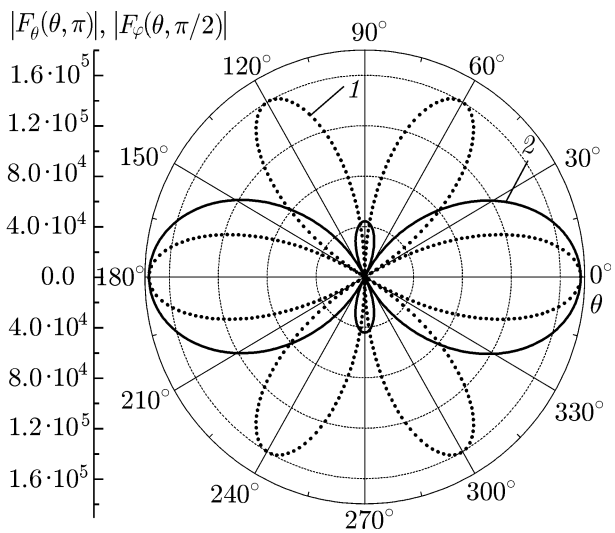

Fig. 4. Scattering patterns for the sphere with $\varepsilon = -1.335$ and $\mu = -1$ at the dimensionless frequency $ka_3 = 0.2046\ldots$: curves *1* and *2* correspond to $F_\theta(\theta,0)$ and $F_\varphi(\theta,\pi/2)$, respectively.

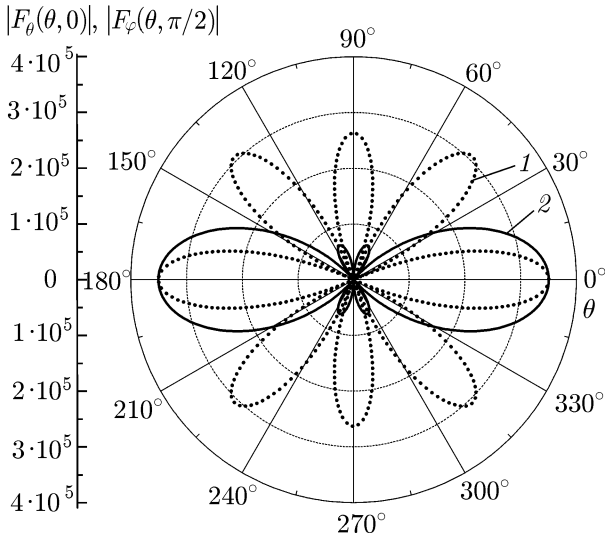

Fig. 5. Scattering patterns for the sphere with $\varepsilon = -1.252$ and $\mu = -1$ at the dimensionless frequency $ka_4 = 0.3494\ldots$: curves *1* and *2* correspond to $F_\theta(\theta,0)$ and $F_\varphi(\theta,\pi/2)$, respectively.

loss in the medium. One can see in the figure that an increase in the thermal loss leads to a decrease in the resonance Q-factor Q_3. Curve *1* in this figure, which corresponds to $\nu = 10^{-9}$, coincides almost completely with curve *1* in Fig. 2, which corresponds to the absence of the thermal loss when $Q_3 \sim 5\cdot10^4$. At $\nu = 10^{-5}$, the Q-factor decreases until it reaches the value $Q_3 \approx 2\cdot10^2$.

Figure 4 shows the absolute values of the components $F_\theta(\theta,0)$ and $F_\varphi(\theta,\pi/2)$ of the vector scattering pattern at the resonant frequency ka_3. The component F_θ contains six lobes that are nearly identical. The component F_φ has two symmetric main lobes which are oriented in the directions $\theta = 0$ and $\theta = \pi$. Figure 5 shows the absolute values of the components F_θ and F_φ at the resonant dimensionless frequency ka_4. In this case, the F_θ component has eight lobes, and the F_φ component is still characterized by two main lobes. This form of the radiation patterns corresponds to analytical expressions (48).

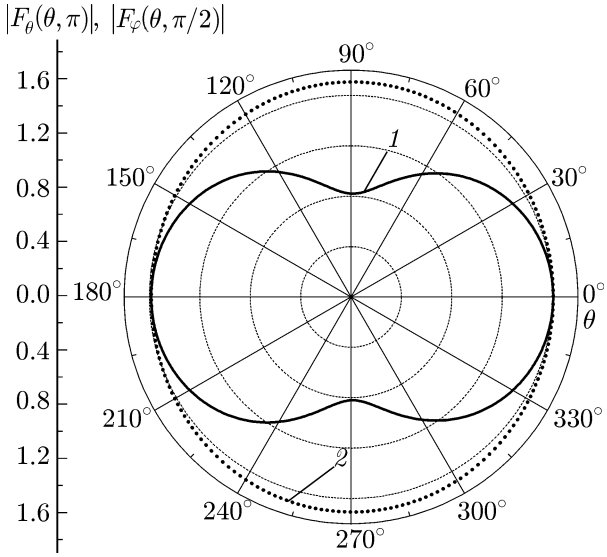

Fig. 6. Scattering patterns for the sphere with $\varepsilon = -1.3$ and $\mu = -1$ at the dimensionless frequency $ka_3 = 0.2046\ldots$: curves *1* and *2* correspond to $F_\theta(\theta, 0)$ and $F_\varphi(\theta, \pi/2)$, respectively.

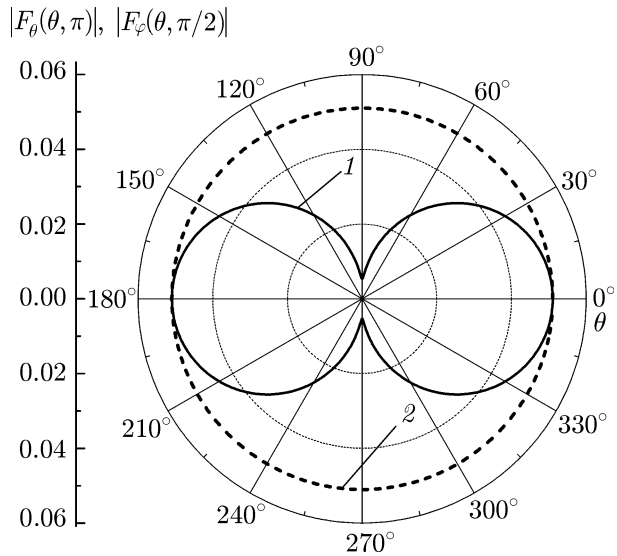

Fig. 7. Scattering patterns for the sphere with $\varepsilon = 1.3$ and $\mu = 1$ at the dimensionless frequency $ka_3 = 0.2046\ldots$: curves *1* and *2* correspond to $F_\theta(\theta, 0)$ and $F_\varphi(\theta, \pi/2)$, respectively.

Let us compare the resonance properties of a small sphere with analogous properties of the narrow cylinder [8]. Recall that within the framework of the two-dimensional problem of diffraction by a cylinder, low-frequency resonances occur for ε close to -1 (in the case of TM polarization). This condition is mandatory for all values of the azimuthal index m of the resonance oscillations (at the resonance, the dependence of the field on the angle φ is determined by the term $\cos(m\varphi)$). In a sphere, resonances of the electric-type modes occur for ε close to $-(l+1)/l$, where $l = 1, 2, 3, \ldots$. Note that $2l$ is equal to the number of lobes in the radiation pattern $F_\theta(\theta, 0)$. Thus, the index l in the three-dimensional problem of a sphere acts as the index m in the two-dimensional problem of a cylinder.

The frequency-amplitude characteristic of the cylinder at a given value of ε is a sequence of resonance bursts with different indices m corresponding to each burst. The frequency-amplitude characteristic of a sphere contains a single resonance and the index l, which is predetermined by the choice of the value of ε, corresponds to it. Curves *1* and *2* in Fig. 2 represent the resonance frequency-amplitude characteristics of the sphere for $\varepsilon \approx -4/3$ and $\varepsilon \approx -5/4$, respectively. If the dielectric permittivity is specified arbitrarily, quasistatic resonances will not exist, generally speaking, which is demonstrated by curve *3* in Fig. 2 for $\varepsilon = -1.3$ and $\mu = -1$

Figure 6 shows the scattering patterns F_θ and F_φ for a metamaterial sphere with $\varepsilon = -1.3$ and $\mu = -1$ at the dimensionless frequency $ka_3 = 0.204\ldots$, which is the resonant frequency in the case where $\varepsilon = -1.335$ and $\mu = -1$. Recall that these patterns are normalized to the maximum amplitude of the radiation patterns $|F_\theta^0|$ and $|F_\varphi^0|$ of the primary field. The patterns presented in Fig. 6 are not directional, and their amplitudes decreased by more than 10^5 times compared with the resonance case (see Fig. 4). Nevertheless, the amplitudes of the patterns exceed unity, which means that the effect of the nonresonance field enhancement is present [10]. Enhancement of the source field compared with the field in the absence of the scatterer (at the same value of the current supplied) occurs in a wide frequency range (see Fig. 2) and is observed only in the case of diffraction by metamaterial bodies. For comparison, Fig. 7 shows patterns of scattering by a dielectric sphere. The electrical size of the sphere and the refractive index of the material are chosen such as to ensure their coincidence with similar parameters of the above-considered metamaterial sphere ($\varepsilon = 1.3$, $\mu = 1$, and $ka = 0.204\ldots$) with accuracy up to one decimal place. One can see that the absolute values of the scattering patterns are much smaller than unity, which indicates that the field enhancement effect is absent in this case. Then the scattering patterns have the form identical to those of

the radiation patterns of the primary field (see Eqs. (39) and (40)). The frequency-amplitude characteristic of the dielectric sphere in a wide frequency range is represented by curve *4* in Fig. 2. It follows from the comparison of curves *3* and *4* in Fig. 2 that the amplitude of the scattered field for a metamaterial sphere is almost two orders of magnitude higher than that in the case of a dielectric sphere.

Finally, it should be noted that resonance excitation of the magnetic-type modes occurs when the magnetic permeability of the sphere is close to the value $\mu = -(l+1)/l$, where $l = 1, 2, 3, \ldots$. At resonance, the components of the vector scattering pattern will be described by the functions

$$F_\theta \sim \cos\varphi \frac{P_l^1(\cos\theta)}{\sin\theta}, \qquad F_\varphi \sim -\sin\varphi \frac{\mathrm{d}P_l^1(\cos\theta)}{\mathrm{d}\theta}. \tag{65}$$

The calculations performed for the case $\varepsilon = -1$ and $\mu = -1.335$ (cf. Eq. (44)) showed that at the resonant dimensionless frequency ka_3, the patterns F_θ and F_φ have the same form as the patterns in Fig. 4 to an accuracy of the replacements $F_\theta \to F_\varphi$ and $F_\varphi \to F_\theta$. In this case, the field amplitude turned out to be an order of magnitude lower.

7. CONCLUSIONS

We have studied numerically the properties of the electromagnetic fields which arise when a meridional electric dipole excites a sphere made of a metameterial. The regions of electrodynamic parameters for which high-Q quasistatic resonances exist have been established. It is shown that frequency characteristics are essentially different for three- and two-dimensional metamaterial objects. It was found that the scattering patterns at resonance are of multi-lobe form, which is typical of superdirective antennas. The influence of the thermal loss on the resonance Q-factors has been studied. The effect of nonresonance enhancement of the scattered field has been found.

This work was partially supported by the Russian Foundation for Basic Research (project No. 12–02–00062-a).

REFERENCES

1. V. G. Veselago, *Sov. Phys. Uspekhi* [in Russian], **10**, 509 (1968).
2. A. Sihvola, *Metamaterials*, **1**, No. 1, 2 (2007).
3. K. Yu. Bliokh and Yu. P. Bliokh, *Physics — Uspekhi*, **47**, No. 4, 393 (2004).
4. D. R. Smith, J. B. Pendry, and M. C. K. Wiltshire, *Science*, **305**, 788 (2004).
5. A. A. Zharov, I. G. Kondrat'ev, and A. I. Smirnov, *Radiophys. Quantum Electron.*, **48**, Nos. 10–11, 871 (2005).
6. V. V. Klimov, *Nanoplasmonics* [in Russian], Fizmatlit, Moscow (2009).
7. A. P. Anyutin, I. P. Korshunov, and A. D. Shatrov, in: *Proc. 7th Int. Congress on Advanced Electromagnetic Materials in Microwaves and Optics (META'2013), Bordeaux, France, 2013.*
8. A. P. Anyutin, I. P. Korshunov, and A. D. Shatrov, *J. Commun. Technol. Electron.*, **59**, No. 7, 704 (2014).
9. A. P. Anyutin, I. P. Korshunov, and A. D. Shatrov, *J. Commun. Technol. Electron.*, **58**, No. 9, 926 (2013).
10. A. P. Anyutin, I. P. Korshunov, and A. D. Shatrov, *JETP*, **118**, No. 1, 27 (2014).
11. M. Born and E. Wolf, *Principles of Optics*, Cambridge Univ. Press, Cambridge (2003).
12. G. T. Markov and A. F. Chaplin, *Excitation of Electromagnetic Waves* [in Russian], Radio i Svyaz', Moscow (1983).

13. M. Abramowitz and I. A. Stegun, eds., *Handbook of Mathematical Functions with Formulas, Graphs, and Mathematical Tables*, Dover, New York (1972).

14. A. G. Kyurkchan and D. B. Demin, *J. Commun. Technol. Electron.*, **49**, No. 11, 1218 (2004).

15. A. G. Kyurkchan and D. B. Demin, *J. Quant. Spectrosc. Radiat. Transfer*, **89**, 237 (2004).